Hardware-Efficient Autonomous Quantum Memory Protection

Zaki Leghtas,[1,2] Gerhard Kirchmair,[2,3,4] Brian Vlastakis,[2] Robert J. Schoelkopf,[2]
Michel H. Devoret,[2] and Mazyar Mirrahimi[1,2]

[1]*INRIA Paris-Rocquencourt, Domaine de Voluceau, Boîte Postale 105, 78153 Le Chesnay Cedex, France*
[2]*Department of Applied Physics, Yale University, New Haven, Connecticut 06520, USA*
[3]*Institut für Experimentalphysik, Universität Innsbruck, Technikerstraße 25, A-6020 Innsbruck, Austria*
[4]*Institut für Quantenoptik und Quanteninformation, Österreichische Akademie der Wissenschaften, Otto-Hittmair-Platz 1, A-6020 Innsbruck, Austria*

(Received 20 May 2013; published 20 September 2013)

We propose to encode a quantum bit of information in a superposition of coherent states of an oscillator, with four different phases. Our encoding in a single cavity mode, together with a protection protocol, significantly reduces the error rate due to photon loss. This protection is ensured by an efficient quantum error correction scheme employing the nonlinearity provided by a single physical qubit coupled to the cavity. We describe in detail how to implement these operations in a circuit quantum electrodynamics system. This proposal directly addresses the task of building a hardware-efficient quantum memory and can lead to important shortcuts in quantum computing architectures.

DOI: 10.1103/PhysRevLett.111.120501 PACS numbers: 03.67.Pp, 85.25.−j

Long lived coherence is a prerequisite for quantum computation. A promising software solution to extend the coherence time of a quantum bit of information is quantum error correction (QEC) [1,2]. In the field of circuit quantum electrodynamics, the last decade has seen impressive improvements in the coherence times of qubits and cavities, thus reaching the quality threshold needed for QEC to be effective [3]. The usual approach for the realization of QEC is to use many qubits to obtain a larger Hilbert space of the qubit register. In this Hilbert space of larger dimension, one can then redundantly encode the quantum information in a manner that makes QEC tractable: different error channels lead to distinguishable syndromes. There are two major drawbacks of using multiqubit registers. The first one is fundamental: with each added qubit, several new decoherence channels are added. This multiplies the number of possible errors and requires measuring more error syndromes. The second is practical: it still seems extremely challenging to build a register of more than on the order of 10 qubits.

In this Letter, we take an orthogonal direction which constitutes a complete change of paradigm. Our approach is to use a cavity mode, namely, a harmonic oscillator, as a protected quantum memory, hence replacing the multiqubit register by a single cavity mode. The latter is an infinite dimensional system and provides a vast Hilbert space to redundantly encode quantum information. The power of this idea lies in the fact that the dominant decoherence channel in a cavity is photon damping, and no more channels are added if we increase the number of photons we insert in the cavity. Hence, only a single error syndrome needs to be measured to identify if an error has occurred or not. This key property of the harmonic oscillator is a direct consequence of its linearity. This, on the other hand, comes at a high price: such a linear system is not easily controllable and using classical drives, one can only prepare coherent states in the cavity. However, resonantly coupling a qubit to a cavity has led to the preparation of arbitrary states of the cavity [4]. Moreover, it is known that dispersively coupling a qubit to a cavity aids the manipulation of the cavity state [5,6], and we have recently shown that it leads to a very strong controllability over its Hilbert space: we can prepare any superposition of quasiorthogonal coherent states [7]. Making use of the three properties of controllability, a single decoherence channel, and minimal hardware, we can realize a protected quantum memory with currently available devices. Moreover, we provide a detailed sequence of operations which encode the quantum information in the cavity, protect it, and decode it back to a qubit. We also provide a simple extension of our scheme which protects against multiple jumps in the cavity.

In our scheme (see Fig. 1), the logical qubit is encoded in a multicomponent superposition of coherent states in the cavity mode [8]. This simple cavity-qubit system is the standard building block of both circuit and cavity quantum electrodynamics (QED) experiments [9]. A cavity mode is thus a powerful piece of hardware for storing and protecting quantum information [10–12].

An arbitrary qubit state $c_g|g\rangle + c_e|e\rangle$ (we denote $|g\rangle$ and $|e\rangle$ the ground and excited states) is mapped into a multicomponent coherent state $|\psi_\alpha^{(0)}\rangle = c_g|\mathcal{C}_\alpha^+\rangle + c_e|\mathcal{C}_{i\alpha}^+\rangle$, where

$$|\mathcal{C}_\alpha^\pm\rangle = \mathcal{N}(|\alpha\rangle \pm |-\alpha\rangle),$$
$$|\mathcal{C}_{i\alpha}^\pm\rangle = \mathcal{N}(|i\alpha\rangle \pm |-i\alpha\rangle).$$

$\mathcal{N}$ ($\approx 1/\sqrt{2}$) is a normalizing factor, and $|\alpha\rangle$ denotes a coherent state of complex amplitude α, chosen such that $|\alpha\rangle$, $|-\alpha\rangle$, $|i\alpha\rangle$, and $|-i\alpha\rangle$ are quasiorthogonal, i.e.,

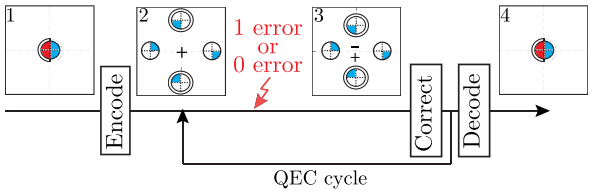

FIG. 1 (color online). Our AQEC scheme is composed of three operations: encoding, correcting, and decoding. The joint cavity-qubit state is represented by a generalized Fresnel diagram. Fresnel plane positions carry the description of the cavity mode, while colors carry the description of the qubit. Our protocol only requires that we represent superpositions of coherent states entangled with the qubit degrees of freedom. A circle whose center is positioned at α in the diagram corresponds to a coherent state component of amplitude α. For example, the diagram in frame 2 represents the state $c_g|C_\alpha^+\rangle + c_e|C_{i\alpha}^+\rangle = \mathcal{N}(c_g|g,\alpha\rangle + c_g|g,-\alpha\rangle + c_e|g,i\alpha\rangle + c_e|g,-i\alpha\rangle)$, where $\mathcal{N} \approx 1/\sqrt{2}$ is a normalization factor. Each component of this state corresponds to a circle whose color refers to whether the qubit is in $|g\rangle$ (blue areas) or $|e\rangle$ (red areas). The rim of each circle indicates whether the prefactor is c_g (single line) or c_e (double line). Finally, the fraction of the colored disk represents the total weight $|\mathcal{N}c_{g,e}|^2$ of each coherent component. Here, quarter filled circles correspond to $|\mathcal{N}c_{g,e}|^2 = 1/4$. Initially (frame 1), the qubit is in $c_g|g\rangle + c_e|e\rangle$ and the cavity is in vacuum. The plus (respectively, minus) sign in the 2 and 3 diagrams indicates whether the logical qubit is encoded in an even (respectively, odd) cavity state. A jump from a plus to a minus sign is induced by a photon loss error, which we aim to correct.

$|\langle\alpha|i\alpha\rangle|^2 \ll 1$ (note that for $\alpha = 2$, $|\langle\alpha|i\alpha\rangle|^2 < 10^{-3}$). An important contribution of this Letter is to propose a detailed sequence of operations which deterministically and efficiently realizes the unitary operation

$$\mathcal{U}_{\text{encode}}(c_g|g\rangle + c_e|e\rangle) \otimes |0\rangle = |g\rangle \otimes (c_g|\mathcal{C}_\alpha^+\rangle + c_e|\mathcal{C}_{i\alpha}^+\rangle) + O(e^{-|\alpha|^2}) \quad \forall\ c_g, c_e.$$

The error term $O(e^{-|\alpha|^2})$ is due to the fact that the two states $|\mathcal{C}_\alpha^+\rangle$ and $|\mathcal{C}_{i\alpha}^+\rangle$ are not exactly orthogonal. However, this error term decreases exponentially with photon number $|\alpha|^2$ and can rapidly be neglected compared to the efficiency of our gate. Similarly, we perform the inverse operation $\mathcal{U}_{\text{decode}}$, mapping back the quantum state of the cavity to the physical qubit. Before presenting the scheme which performs the above unitary operations, let us show how this encoding protects against photon loss.

Together with $|\psi_\alpha^{(0)}\rangle$, we introduce $|\psi_\alpha^{(1)}\rangle = c_g|\mathcal{C}_\alpha^-\rangle + ic_e|\mathcal{C}_{i\alpha}^-\rangle$, $|\psi_\alpha^{(2)}\rangle = c_g|\mathcal{C}_\alpha^+\rangle - c_e|\mathcal{C}_{i\alpha}^+\rangle$, and $|\psi_\alpha^{(3)}\rangle = c_g|\mathcal{C}_\alpha^-\rangle - ic_e|\mathcal{C}_{i\alpha}^-\rangle$. The logical 0, $|\mathcal{C}_\alpha^+\rangle$, and the logical 1, $|\mathcal{C}_{i\alpha}^+\rangle$, have the three following remarkable properties. First, the states $|\psi_\alpha^{(n)}\rangle$ evolve after a quantum jump due to a photon loss, to $\mathbf{a}|\psi_\alpha^{(n)}\rangle / \| \mathbf{a}|\psi_\alpha^{(n)}\rangle \| = |\psi_\alpha^{[(n+1)\text{mod}4]}\rangle$, where $\mathbf{a}$ is the annihilation operator. Therefore, the set $\{|\psi_\alpha^{(n)}\rangle\}$ is closed under the action of $\mathbf{a}$. Second, in the absence of jumps during a time interval t, $|\psi_\alpha^{(n)}\rangle$ deterministically evolves to $|\psi_{\alpha e^{-\kappa t/2}}^{(n)}\rangle$, where κ is the cavity decay rate. Third, defining the parity operator $\Pi = \exp(i\pi\mathbf{a}^\dagger\mathbf{a})$, we have $\langle\psi_\alpha^{(n)}|\Pi|\psi_\alpha^{(n)}\rangle = (-1)^n$. The parity operator acts therefore as a quantum jump indicator. Now, suppose we have a quantum non demolition parity measurement, and that we have counted c jumps during a time t, the initial state has evolved to $|\psi_{\alpha e^{-\kappa t/2}}^{(c\text{mod}4)}\rangle$. Using similar operations to those for $\mathcal{U}_{\text{encode}}$, we obtain a unitary transformation, independent of c_g and c_e, which maps $|\psi_{\alpha e^{-\kappa t/2}}^{(c\text{mod}4)}\rangle$ back to $|\psi_\alpha^{(0)}\rangle$, therefore undoing the effect of decoherence caused by random quantum jumps and repumping the decayed energy back into the cavity.

Such a measurement based QEC (MBQEC) [13] (see the Supplemental Material [14]) requires fast and reliable measurements which would necessitate employing quantum limited amplifiers. Here, we introduce an autonomous QEC (AQEC) scheme, avoiding the need of such resources. Instead, it requires the availability of a rapid, high fidelity qubit reset. Depending on the experimental setting, either one method or the other could be preferred.

AQEC [15–17] is realized by using an auxiliary quantum system that we take here to be the same coupled physical qubit, which is used to manipulate the cavity state. The idea consists in finding a unitary operation $\mathcal{U}_{\text{correct}}$ such that

$$\begin{aligned}\mathcal{U}_{\text{correct}}:\ |g\rangle \otimes |\mathcal{C}_{\alpha e^{-\kappa t/2}}^{\pm}\rangle &\to \frac{1}{\sqrt{2}}(|g\rangle \pm |e\rangle) \otimes |\mathcal{C}_\alpha^+\rangle,\\ |g\rangle \otimes |\mathcal{C}_{i\alpha e^{-\kappa t/2}}^{\pm}\rangle &\to \frac{1}{\sqrt{2}}(|g\rangle \pm |e\rangle) \otimes |\mathcal{C}_{i\alpha}^+\rangle,\end{aligned} \tag{1}$$

neglecting terms of order $e^{-|\alpha|^2}$ due to the nonorthogonality of the coherent states. This unitary operation transfers the entropy of the quantum system to be protected to the auxiliary one. Now, resetting the state of the auxiliary system, we can evacuate the entropy, restoring the initial full state.

More precisely, we encode the qubit state $c_g|g\rangle + c_e|e\rangle$ in the state $|\psi_\alpha^{(0)}\rangle$ and, in a stroboscopic manner, perform the above unitary transformation followed by the qubit reset. Assuming that at most one quantum jump can happen between two correction operations separated by time T_w, the state before the correction is given either by $|\psi_{\alpha e^{-\kappa T_w/2}}^{(0)}\rangle$ or $|\psi_{\alpha e^{-\kappa T_w/2}}^{(1)}\rangle$. After the correction operation, we have restored the initial state $|\psi_\alpha^{(0)}\rangle$.

The operations involved in the encoding, decoding, and correction rely on three unitary transformations. The first one D_α displaces the cavity state by a complex amplitude α regardless of the qubit state. Second, the conditional cavity phase shift Π (respectively, $\sqrt{\Pi}$) transforms states of the form $|e,\alpha\rangle$ to $|e,-\alpha\rangle$ (respectively, $|e,i\alpha\rangle$) and leaves $|g,\alpha\rangle$ unchanged. Third, a conditional qubit rotation $X_{\theta,\eta}^0$ rotates the qubit state by $e^{\theta/2(e^{i\eta}|e\rangle\langle g| - e^{-i\eta}|g\rangle\langle e|)}$ only if

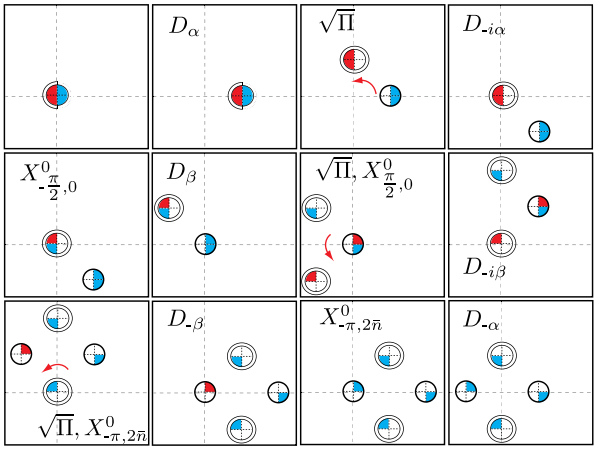

FIG. 2 (color online). Sequence of operations which generate $\mathcal{U}_{\text{encode}}$. See the caption of Fig. 1 for an explanation of the diagram notation. The symbol given in the kth frame corresponds to the operation performed to go from frame $k-1$ to k. The curved arrow corresponds to the rotation of the excited state component of the state. We denote $\beta = \alpha(-1+i)$ and $\bar{n} = |\alpha|^2$. The frames are ordered from left to right and top to bottom.

the cavity is in the vacuum state $|0\rangle$. See Fig. 2 for a detailed illustration of how combining these operations leads to the encoding gate. Note that for some rotations, η takes the value $2\bar{n}$ in order to compensate the phase accumulated due to the previous displacement [see Ref. [18], Eq. (3.50)]. A circuit representation of the sequence of operations for the encoding and the decoding gates is given in the Supplemental Material [14]. We have already successfully implemented, in our laboratory, a sequence of operations similar to this encoding operation, and the experimental results will be presented elsewhere [19]. The correction operation also requires a qubit reset that forces the qubit state to $|g\rangle$ independently of the cavity state. See Fig. 3 for a detailed illustration of the correction operation. In the proposed scheme, we have introduced the qubit reset in the middle, in contrast with what is suggested in Eq. (1). We find the resulting sequence to be more efficient.

We now quantify the performance of our AQEC scheme. Let $\rho_\alpha^{(n)}$ denote the projector onto the state $|\psi_\alpha^{(n)}\rangle$. The effect of the waiting time T_w between two corrections may be modeled by a Kraus operator

$$\mathcal{K}_w\colon \rho_\alpha^{(0)} \to p_0\rho_{\tilde{\alpha}}^{(0)} + p_1\rho_{\tilde{\alpha}}^{(1)} + p_2\rho_{\tilde{\alpha}}^{(2)} + p_3\rho_{\tilde{\alpha}}^{(3)},$$

where $\tilde{\alpha} = \alpha e^{-\kappa T_w/2}$. For a Poisson process with a jump rate λ_{jump}, the probability of having k jumps during a time interval T_w is given by $\exp(-\lambda_{\text{jump}}T_w)\lambda_{\text{jump}}^k T_w^k/k!$. We denote as p_k the probability of having k (mod 4) jumps during the waiting time T_w. In the limit where $\epsilon_{\text{jump}} \equiv \lambda_{\text{jump}}T_w = \kappa T_w\bar{n} \ll 1$, we have $p_0 \approx 1 - \epsilon_{\text{jump}} + \epsilon_{\text{jump}}^2/2$, $p_1 \approx \epsilon_{\text{jump}} - \epsilon_{\text{jump}}^2$, and $p_2 + p_3 \approx \epsilon_{\text{jump}}^2/2$.

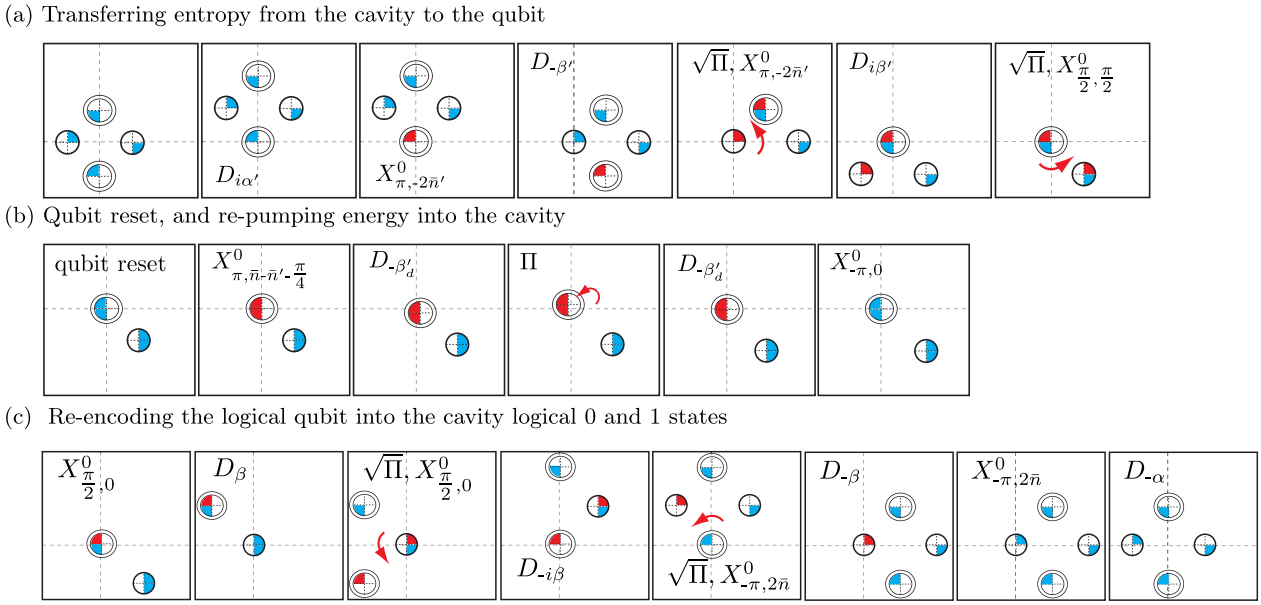

FIG. 3 (color online). (a)–(c) Full correcting sequence obtained by concatenating the three sequences of pulses. (a) The entropy is transferred from the cavity to the qubit. (b) First, the qubit is reset to its ground state and then energy is repumped into the coherent component to compensate the deterministic decay due to damping during the waiting time T_w between two correction sequences. (c) The cavity state is mapped back onto the initial cavity logical 0 and logical 1. See the caption of Fig. 1 for an explanation of the diagram notation. Here, we denote $\alpha' = e^{-\kappa T_w/2}\alpha$ the damped amplitude after the waiting time T_w, $\bar{n}' = |\alpha'|^2$, and $\beta' = \alpha'(i-1)$. In order to compensate the damping during T_w, during the repumping step, we take $\beta'_d = (\beta' - \beta)/2$. In the last frame of (a), the error is encoded in the phase of the qubit superposition and is not represented in this diagram. After qubit reset [first frame of (b)], this phase information is erased.

The correction step consists of the joint unitary operation on the cavity-qubit system followed by the qubit reset. We model the effect of this operation by the Kraus operator $\mathcal{K}_c$, mapping both $|\psi^{(0)}_{\alpha e^{-\kappa T_w/2}}\rangle$ and $|\psi^{(1)}_{\alpha e^{-\kappa T_w/2}}\rangle$ to $|\psi^{(0)}_{\alpha}\rangle$. After N correction cycles and waiting times (each one taking a time $T_c + T_w$), we obtain a fidelity at time $t_N = N(T_c + T_w)$: $F_{\mathrm{AQEC}}(t_N) = \mathrm{Tr}[\rho^{(0)}_{\alpha}(\mathcal{K}_c\mathcal{K}_w)^N\rho^{(0)}_{\alpha}]$.

We denote $(1 - \epsilon_{\mathrm{correct}})$ as the fidelity of the correction operation, taking into account various imperfections and particularly finite coherence times and finite pulse lengths. Also, $\epsilon_{\mathrm{wait}} = \epsilon^2_{\mathrm{jump}}/2$ denotes the probability of having two or more jumps during the waiting time between two correction steps. We have $F_{\mathrm{AQEC}}(t_N) \approx [(1 - \epsilon_{\mathrm{correct}})(1 - \epsilon_{\mathrm{wait}})]^N$. Assuming $T_c \ll T_w$, we obtain an effective decay rate $\kappa^{\mathrm{AQEC}}_{\mathrm{eff}} \approx [\epsilon_{\mathrm{correct}} + (\kappa T_w \bar{n})^2/2]/T_w$. The latter is maximal for $T_w = \sqrt{2\epsilon_{\mathrm{correct}}}/\kappa\bar{n}$, which would lead to

$$\kappa^{\mathrm{AQEC}}_{\mathrm{eff}} = \kappa\bar{n}\sqrt{2\epsilon_{\mathrm{correct}}}. \quad (2)$$

This is an improvement by a factor of $1/\sqrt{2\epsilon_{\mathrm{correct}}}$ with respect to the decay rate $\kappa\bar{n}$ of $|\psi^{(0)}_{\alpha}\rangle$ in the absence of correction. Indeed, considering an architecture represented in Fig. 4 and the parameters introduced in Sec. 1 of the Supplemental Material [14] leads to an improvement of about 1 order of magnitude. We even find an improvement of a factor of $\sim$2 with respect to the lifetime of a single photon in the cavity. This proves that this scheme can be more effective than simply encoding the qubit state in the 0 and 1 Fock states of a cavity using a swap operation [20,21]. Notice that while $\kappa^{\mathrm{AQEC}}_{\mathrm{eff}}$ increases linearly with $\bar{n}$, the error due to the nonorthogonality of the code word decreases exponentially with $\bar{n}$. Hence, a compromise between these two effects is reached for small values of $\bar{n}$.

Here, we show how we could perform our AQEC in practice (see Fig. 4 for a possible implementation of this proposal). We place ourselves in the strong dispersive regime, where both the qubit and the resonator transition

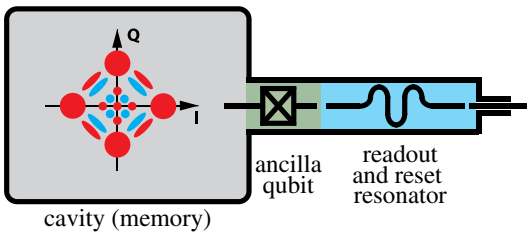

FIG. 4 (color online). Diagram of our proposal to store a quantum bit of information in a single cavity mode. The information is encoded in a superposition of cat states, represented by the I-Q diagram. The cross symbolizes a superconducting qubit. The wavy line represents the readout resonator which measures and resets the ancilla qubit state. This hardware-efficient quantum memory could significantly reduce the complexity of quantum computing architectures.

frequencies split into well-resolved spectral lines indexed by the number of excitations in the qubit and the resonator [22]. The resonator frequency ω_r splits into two well-resolved lines ω^g_r and ω^e_r, corresponding to the cavity's frequency when the qubit is in the ground ($|g\rangle$) or the excited ($|e\rangle$) state. Through the same mechanism, the qubit frequency ω_q splits into $\{\omega^n_q\}_{n=0,1,2,\ldots}$, corresponding to the qubit frequency when the cavity is in the photon number state $|n\rangle$. Recent experiments have shown dispersive shifts that are more than 3 orders of magnitude larger than the qubit and cavity linewidths [23].

The Hamiltonian of such a dispersively coupled qubit-cavity system is well approximated by

$$\mathbf{H}_0 = \omega_q\frac{\boldsymbol{\sigma}_z}{2} + \omega_c\mathbf{a}^\dagger\mathbf{a} - \chi\frac{\boldsymbol{\sigma}_z}{2}\mathbf{a}^\dagger\mathbf{a},$$

where ω_q and ω_c are, respectively, the qubit and cavity frequencies, χ is the dispersive coupling, and $\boldsymbol{\sigma}_z = |e\rangle\times\langle e| - |g\rangle\langle g|$. This Hamiltonian may be written in an appropriate rotating frame as $\mathbf{H} = -\chi|e\rangle\langle e|\mathbf{a}^\dagger\mathbf{a}$. This dispersive coupling is called strong when $\chi \gg \kappa, 1/T_2$, where T_2 is the qubit dephasing time.

As detailed in Ref. [7], the strong dispersive cavity-qubit coupling allows us to efficiently perform conditional qubit rotations, unconditional cavity displacements, and conditional cavity phase shifts. Long selective qubit pulses with carrier frequency ω^0_q can rotate the qubit state conditioned on the cavity being in the vacuum state. Short unselective pulses on the cavity will displace it regardless of the qubit state, and simply waiting for a time π/χ [respectively, $\pi/(2\chi)$] realizes the conditional cavity phase shift Π [respectively, $\sqrt{\Pi}$]. Finally, the qubit reset could be done by rapidly tuning (e.g., with a flux bias line) the qubit frequency to bring it into resonance with a low-Q cavity mode [16]. This operation needs to be fast compared to χ to avoid reentanglement of the qubit to the cavity mode. Another possibility, avoiding fast frequency tuning, is to perform a dynamical cooling cycle, as proposed in Ref. [24].

We have shown that it is possible to protect a logical qubit against relaxation by encoding it in a single cavity coupled to a single physical qubit and driving them with simple control pulses. No control over the qubit frequency or the cavity-qubit coupling is necessary, as long as this coupling is in the strong dispersive regime. Our theoretical prediction of the lifetime improvement is confirmed by numerical simulations of the proposed protocol (see Sec. 1 of the Supplemental Material [14]). Furthermore, we have already successfully prepared, in our laboratory, the state $\mathcal{N}(|C^+_\alpha\rangle + |C^-_\alpha\rangle)$, using a sequence of operations similar to $\mathcal{U}_{\mathrm{encode}}$ [19]. Additional control of the qubit frequency in real time could lead to simpler and faster operations with higher fidelities [25].

This work was partially supported by the French "Agence Nationale de la Recherche" under Project EPOQ2 No. ANR-09-JCJC-0070, the Army Research

Office (ARO) under Project No. ARO-W911NF-09-1-0514, and the NSF DMR-1004406. B. V. acknowledges support from the National Science Foundation, Project No. PHY-0969725.

[1] P. W. Shor, Phys. Rev. A **52**, R2493 (1995).
[2] A. M. Steane, Phys. Rev. Lett. **77**, 793 (1996).
[3] C. Rigetti, S. Poletto, J. Gambetta, B. Plourde, J. Chow, A. Corcoles, J. Smolin, S. Merkel, J. Rozen, G. Keefe *et al.*, Phys. Rev. B **86**, 100506(R) (2012).
[4] M. Hofheinz, H. Wang, M. Ansmann, R. Bialczak, E. Lucero, M. Neeley, A. O'Connell, D. Sank, J. Wenner, J. Martinis *et al.*, Nature (London) **459**, 546 (2009).
[5] M. Brune, E. Hagley, J. Dreyer, X. Maître, A. Maali, C. Wunderlich, J. M. Raimond, and S. Haroche, Phys. Rev. Lett. **77**, 4887 (1996).
[6] C. Guerlin, J. Bernu, S. Deléglise, C. Sayrin, S. Gleyzes, S. Kuhr, M. Brune, J.-M. Raimond, and S. Haroche, Nature (London) **448**, 889 (2007).
[7] Z. Leghtas, G. Kirchmair, B. Vlastakis, M. H. Devoret, R. J. Schoelkopf, and M. Mirrahimi, Phys. Rev. A **87**, 042315 (2013).
[8] W. Zurek, Nature (London) **412**, 712 (2001).
[9] R. J. Schoelkopf and S. Girvin, Nature (London) **451**, 664 (2008).
[10] D. Gottesman, A. Kitaev, and J. Preskill, Phys. Rev. A **64**, 012310 (2001).
[11] D. Vitali, P. Tombesi, and G. J. Milburn, Phys. Rev. A **57**, 4930 (1998).
[12] S. Zippilli, D. Vitali, P. Tombesi, and J. M. Raimond, Phys. Rev. A **67**, 052101 (2003).
[13] J. Chiaverini, D. Leibfried, T. Schaetz, M. Barrett, R. Blakestad, J. Britton, W. Itano, J. Jost, E. Knill, C. Langer *et al.*, Nature (London) **432**, 602 (2004).
[14] See Supplemental Material at http://link.aps.org/supplemental/10.1103/PhysRevLett.111.120501 for the measurement based version of our QEC protocol, and an extension to higher order QEC.
[15] P. Schindler, J. T. Barreiro, T. Monz, V. Nebendahl, D. Nigg, M. Chwalla, M. Hennrich, and R. Blatt, Science **332**, 1059 (2011).
[16] M. Reed, L. DiCarlo, S. Nigg, L. Sun, L. Frunzio, S. Girvin, and R. Schoelkopf, Nature (London) **482**, 382 (2012).
[17] J. Kerckhoff, H. I. Nurdin, D. S. Pavlichin, and H. Mabuchi, Phys. Rev. Lett. **105**, 040502 (2010).
[18] S. Haroche and J. Raimond, *Exploring the Quantum: Atoms, Cavities and Photons* (Oxford University, New York, 2006).
[19] B. Vlastakis, G. Kirchmair, Z. Leghtas, S. E. Nigg, L. Frunzio, S. M. Girvin, M. Mirrahimi, M. H. Devoret, and R. J. Schoelkopf (in preparation).
[20] X. Maître, E. Hagley, G. Nogues, C. Wunderlich, P. Goy, M. Brune, J. M. Raimond, and S. Haroche, Phys. Rev. Lett. **79**, 769 (1997).
[21] M. Mariantoni, H. Wang, T. Yamamoto, M. Neeley, R. Bialczak, Y. Chen, M. Lenander, A. O. E. Lucero, D. Sank, M. Weides *et al.*, Science **334**, 61 (2011).
[22] D. Schuster, A. Houck, J. Schreier, A. Wallraff, J. Gambetta, A. Blais, L. Frunzio, J. Majer, B. Johnson, M. Devoret *et al.*, Nature (London) **445**, 515 (2007).
[23] H. Paik, D. Schuster, L. Bishop, G. Kirchmair, G. Catelani, A. Sears, B. Johnson, M. Reagor, L. Frunzio, L. Glazman *et al.*, Phys. Rev. Lett. **107**, 240501 (2011).
[24] K. Geerlings, Z. Leghtas, I. M. Pop, S. Shankar, L. Frunzio, R. J. Schoelkopf, M. Mirrahimi, and M. H. Devoret, Phys. Rev. Lett. **110**, 120501 (2013).
[25] C. Caves and A. Shaji, Opt. Commun. **283**, 695 (2010).